High Magnetic Field NMR Studies of LiVGe_2O_6, a quasi 1-D Spin $S = 1$ System

P. Vonlanthen, K. B. Tanaka, Atsushi Goto, W. G. Clark, P. Millet, J. Y. Henry, J. L. Gavilano, H. R. Ott, F. Mila, C. Berthier, et al.

High Magnetic Field NMR Studies of $LiVGe_2O_6$, a quasi 1-D Spin $S = 1$ System.

P. Vonlanthen,[1] K. B. Tanaka,[1] Atsushi Goto,[1,2] W. G. Clark,[1] P. Millet,[3] J. Y. Henry,[4] J. L. Gavilano,[5] H. R. Ott,[5] F. Mila,[6] C. Berthier,[7] M. Horvatic,[7] Yo Tokunaga,[7] P. Kuhns,[8] A. P. Reyes,[8] and W. G. Moulton[8]

[1]*Department of Physics and Astronomy, University of California at Los Angeles, Los Angeles, CA 90095-1547, U.S.A.*
[2]*National Institute for Materials Science, Tsukuba, Ibaraki 305-0003 JAPAN*
[3]*Centre d'Elaboration des Matériaux et d'Etudes Structurales, 29 rue J. Marvig, 31055 Toulouse Cedex, France*
[4]*Centre d'Etudes Nucléaires, DRFMC/SPSMS/MDN, F-38054 Grenoble Cedex 9, France*
[5]*Laboratorium für Festkörperphysik, ETH-Hönggerberg, CH-8093 Zürich, Switzerland*
[6]*Institut de Physique Théorique, Université de Lausanne, 1015 Lausanne, Switzerland*
[7]*Grenoble High Magnetic Field Laboratory, BP 166, 38042 Grenoble Cedex 9, France*
[8]*National High Magnetic Field Laboratory, Tallahassee, Florida 32310*

(Dated: October 25, 2018)

We report ^{7}Li pulsed NMR measurements in polycrystalline and single crystal samples of the quasi one-dimensional $S = 1$ antiferromagnet $LiVGe_2O_6$, whose AF transition temperature is $T_N \simeq 24.5$ K. The field (B_0) and temperature (T) ranges covered were 9-44.5 T and 1.7-300 K respectively. The measurements included NMR spectra, the spin-lattice relaxation rate (T_1^{-1}), and the spin-phase relaxation rate (T_2^{-1}), often as a function of the orientation of the field relative to the crystal axes. The spectra indicate an AF magnetic structure consistent with that obtained from neutron diffraction measurements, but with the moments aligned parallel to the c-axis. The spectra also provide the T-dependence of the AF order parameter and show that the transition is either second order or weakly first order. Both the spectra and the T_1^{-1} data show that B_0 has at most a small effect on the alignment of the AF moment. There is no spin-flop transition up to 44.5 T. These features indicate a very large magnetic anisotropy energy in $LiVGe_2O_6$ with orbital degrees of freedom playing an important role. Below 8 K, T_1^{-1} varies substantially with the orientation of B_0 in the plane perpendicular to the c-axis, suggesting a small energy gap for magnetic fluctuations that is very anisotropic.

PACS numbers: 75.30.Kz, 75.50.Ee, 76.60.-k

I. INTRODUCTION

Recently, a new quasi 1-D spin $S = 1$ system, $LiVGe_2O_6$, has been the object of intensive experimental[1,2,3] and theoretical investigations.[4,5,6] It has an antiferromagnetic phase transition at about 25 K and the expected Haldane gap is either absent or strongly suppressed. Quantum chemistry calculations[4] indicate that a second-order splitting Δ_{CF} of the t_{2g} orbitals may play a dominant role in this system. Our new measurements indicate that Δ_{CF} might be much smaller than previously thought,[1] leading to a large uniaxial magnetic anisotropy and orbital fluctuations.

It has been established by neutron diffraction measurements that the low temperature phase has a rather simple, long-range antiferromagnetic order.[3] In this paper, we report the results of a number of different NMR measurements on this material. We also address several important questions about the phase transition which remained open previously, including the order of the phase transition, the size and origin of the energy gap in the magnetic excitation spectrum below the Néel temperature, and the orientation of the magnetic moments in the antiferromagnetic phase. Many of the results reported here were obtained on powder samples. Some of the more recent measurements were made on single crystal samples.

The ^{7}Li NMR measurements we report include NMR spectra, the spin-lattice relaxation rate T_1^{-1}, and the spin-spin relaxation rate T_2^{-1}, at magnetic fields B between 9.0 and 44.5 T and temperatures T over the range 1.7 - 300 K. In spite of various attempts to observe the resonance signal of ^{51}V nuclei above the transition and at the lowest temperatures in the AF-phase, only a tiny spurious signal could be detected in the polycrystalline sample and no signal at all was found in the single crystal samples. The 9.0 T measurements were made at UCLA, the measurements between 23 and 44.5 T were done at the NHMFL in Tallahassee, and measurements at 12 T were performed at the GHMFL in Grenoble. We have extended previous NMR measurements on a polycrystalline powder sample[2] to much lower temperatures as well as to much higher magnetic fields. Furthermore, we present the first NMR measurements on $LiVGe_2O_6$ single crystals as a function of the polar and azimuthal angles, which give new insides on the low temperature behavior of this system, where orbital degrees of freedom seem to play an important role.

This paper is organized as follows. First, we describe the preparation of the samples and the measurement procedures. Then, we present the experimental results and a partial interpretation of some of them. In the subsequent discussion we address issues concerning the magnetic structure, the phase transition, the relaxation rate and the influence of orbital degrees of freedom.

II. SAMPLES AND EXPERIMENTAL METHODS

The $LiVGe_2O_6$ powder sample was prepared as described by Millet *et al.*[1] The single crystal samples were synthesized at the Centre d'Etudes Nucléaires in Grenoble using a flux of GeO_2:$Li_2B_4O_7$ with the molar ratio 8:1. After reducing the V_2O_5 with H_2 and using a slow increase of the temperature up to 720 C, the compound $LiVGe_2O_6$ was obtained with a thermal treatment of the components up to 800 C under Ar with 2 % vol H_2. Then, a mixture of 70 %wt of the flux and 30 %wt of the compound was put in platinum crucible and heated for 1 day at 970 C. After that, it was slowly cooled at the rate of 2 C per hour to 780 C, after which the power to the furnace was switched off and allowed to cool to room temperature. Finally, the products were washed with boiling water. Pale green needles were obtained, the maximum size of which was approximately 1 mm × 0.10 mm × 0.050 mm. The typical dimensions of the samples used for our NMR measurements were 700 μm × 100 μm × 50 μm, which corresponds to a mass of about 15 μg and $\sim 3 \cdot 10^{16}$ ^{7}Li spins. The small NMR coils used for most of the single crystal work were a few turns of 25 μm diameter insulated copper wire wound tightly onto the sample.

$LiVGe_2O_6$ crystallizes in the monoclinic system, space group $P2_1/c$.[1] The chains of VO_6 octahedra are parallel to the c-direction and are connected to their neighbor chains only by two GeO_4 tetrahedra. There is a very small coupling perpendicular to the chains. The Vanadium atoms are located in distorted oxygen octahedra and the three t_{2g} orbitals are split into a low-lying doublet (d_{xy}, d_{yz}) and a single orbital (d_{xz}) at an energy Δ_{CF} above the doublet.

All of the NMR results reported here were performed on the ^{7}Li nuclei using standard spin-echo techniques carried out with a spectrometer and probes built at UCLA. The NMR spectra were obtained by frequency-shifted and summed Fourier transform processing[7] with fixed applied magnetic fields between 9.0 and 44.5 Tesla. Rotation of the field alignment about one axis during the measurements was done by placing the sample and NMR coil on a goniometer platform whose orientation was controlled from the top of the probe. Further rotation about a second axis perpendicular to the goniometer rotation axis was carried out by changing the placement of the coil and sample on the goniometer platform when the probe was out of the cryostat. We estimate that the absolute accuracy of the corresponding angle settings was approximately ±10 deg and that the precision in changing the angle with the goniometer was ±0.5 deg. Part of the uncertainty in the absolute angle was associated with the small size of the samples and part of it from thermal contraction in the goniometer control upon cooling from room temperature to low temperatures.

An unsuccessful attempt was made to observe the ^{51}V NMR signal in a single crystal sample. A thorough search was done by sweeping the resonance frequency in the absence of any external field at 4.2 K as well as sweeping B (aligned along the c-axis) between 0 and 14 T with T in the range 1.5 K-5 K at the fixed frequencies 200, 300 and 550 MHz. We attribute the lack of a signal, which otherwise should have been rather intense, to values of T_1 or T_2 that were less than the approximately 2 μs dead time of the NMR spectrometer. It may be that extending such measurements to much lower T will reveal this ^{51}V signal.

The ^{7}Li T_1^{-1} measurements were performed by first rotating the nuclear magnetization out of equilibrium by a short saturation chain of rf-pulses, then waiting a variable recovery time, t, and finally measuring the integrated spin-echo intensity, $m(t)$. As discussed below, the quadrupolar splitting of the NMR line is very small, about 15 kHz, so that a single exponential form is expected for $m(t)$ as long as all parts of the sample have the same value of T_1^{-1}. To monitor any deviation from the single exponential behavior, we used a stretched exponential to fit our data:

$$m(t) = m_\infty + (m_0 - m_\infty)\exp(-t/T_1)^\beta, \qquad (1)$$

where m_0 and m_∞ are the nuclear magnetization at $t = 0$ just after the saturation sequence and the equilibrium magnetization, respectively. The fit parameter T_1 is the single time that characterizes the recovery of the magnetization. It is the time for the quantity $[m_\infty - m(t)]/[m_\infty - m_0]$ to decay to $1/e$. The exponent β reflects the width of the distribution of relaxation rates. For $\beta = 1$, it corresponds to a single exponential and as β decreases from 1, it represents a progressively broader distribution. The T_1^{-1} measurements were done at Larmor frequencies between 149 and 762 MHz and applied magnetic fields between 9.0 and 41.5 T. For some of the measurements at high magnetic fields below 3 K only the beginning of the recovery curves were measured and the parameter m_∞ was set using values from the measurements between 10 and 3 K and the inverse temperature dependence of m_∞.

Our T_2^{-1} measurements were done at 148.981 MHz in a field of 9.0 T. The pulse sequence used was a $\pi/2$ preparation pulse applied to m_∞ followed a time τ later by a second pulse whose angle was set to maximize the amplitude of the echo. The integral of the spin echo signal was recorded as a function of τ. The decay of the signal was analyzed using the function:

$$m(2\tau) = m(0)\exp -(2\tau/T_2)^\beta, \qquad (2)$$

where β is the stretched exponential parameter between 1 (exponential decay) and 2 (gaussian decay). For the powder sample the β parameter was usually left free during the fit, and resulted in values around 1.4. The spin-echo amplitude for the single crystal measurements was modulated by the quadrupolar interaction, which caused strong deviations of $m(2\tau)$ from an exponential decay. In this case, the value of β used in the analysis was fixed at 2.

III. EXPERIMENTAL RESULTS

A. NMR spectra of polycrystalline $LiVGe_2O_6$

Figure 1 shows two NMR spectra of the powder sample in the paramagnetic regime, i.e. at $T > T_N \approx 25$ K. The experimental points are indicated by the symbols and the solid and dotted lines are fits to a model of a polycrystalline powder in the presence of an axially symmetric, anisotropic shift,[8] as discussed below.

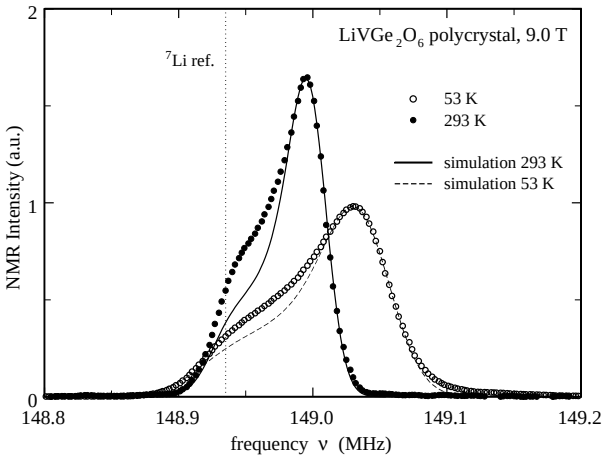

FIG. 1: ^{7}Li NMR spectra in the paramagnetic phase of polycrystalline $LiVGe_2O_6$. The dotted line is the expected position of ^{7}Li in a reference compound like LiCl. The solid and dashed lines are simulations (see text).

For the simulation of the asymmetric NMR spectra in the paramagnetic regime we assumed each V ion to have a moment along the applied magnetic field, whose magnitude is independent of the orientation. Hence, the anisotropy of the g-factor was not taken into account. It was, however, verified that when $1 > g_\perp/g_\parallel \geq 0.5$, results similar to those for an isotropic g-factor are obtained. The corresponding magnetic field at the Li sites was then calculated by adding all the dipole contributions of the V ions in a sphere of about 5 nm diameter around the Li ion. It was verified that modifying the diameter of the sphere does not have any effects on the results. The hyperfine field at the Li sites cannot, however, be fully accounted for by assuming a purely dipolar field of the V moments. An additional isotropic hyperfine coupling of the order of 0.048 T/μ_B is needed. The latter may arise in a manner similar to the superexchange interaction. By assuming a randomly distributed powder, i.e., the direction of the applied magnetic field is pointing along all possible directions of the unit sphere, the Li spectra were then simulated at different temperatures. From the simulations of the measured spectra, one obtains for the average component $< M_Z >$ of the magnetic moments along the direction of the applied field 0.048 μ_B at 300 K and 0.080 μ_B at 53 K, respectively. Their ratio is what one expects from the temperature dependence of the dc-susceptibility.[2] The simulations, shown in Fig. 1 are based on only three parameters: i) an isotropic hyperfine coupling, which is the same for all the data, ii) the size of the magnetic moment on the V ions, whose temperature dependence follows the dc-susceptibility and iii) a gaussian broadening function. In view of the small number of parameters the fits agree fairly well with the measured data. Some deviations are observed in the low frequency part of the signal; their origin is not yet understood.

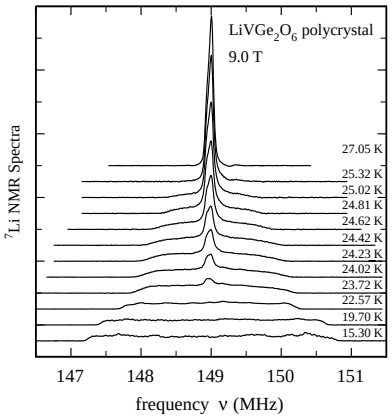

FIG. 2: ^{7}Li NMR spectra of polycrystalline $LiVGe_2O_6$ at 9.0 T for T between 15 and 27 K.

The 9.0 T NMR powder spectra near the transtion and in the ordered phase are shown in Fig. 2. They show a continuous transfer of spectral weight from a narrow line in the paramagnetic phase to a broad signal in the antiferromagnetic (AF) phase that occurs over a narrow temperature range. As seen in Fig. 3, which shows the fraction of the intensity in the AF phase, both phases coexist in a temperature range of about 1.5 K around 24.4 K.

The order parameter of the AF phase is the magnitude and polarization of the AF moments associated with the V atoms. They generate a corresponding magnetic field $\mathbf{B}_i$ at the i-th ^{7}Li sites, which can be calculated for a given AF moment configuration. Depending on the configuration of the AF state, $\mathbf{B}_i$ may have a sequence of values at different ^{7}Li sites or be given by a single value for all of them. At the high magnetic fields used in our experiments, the ^{7}Li spins probe the static order parameter through the shift in their spectrum, which is given by the component of $\mathbf{B}_i$ that is parallel to the applied field $\mathbf{B_0}$. For a randomly-oriented polycrystalline sample, the NMR spectrum in the AF phase depends on the response of the AF polarization to the varying orientation of the external field.

The NMR spectra in the AF phase below 23 K have a

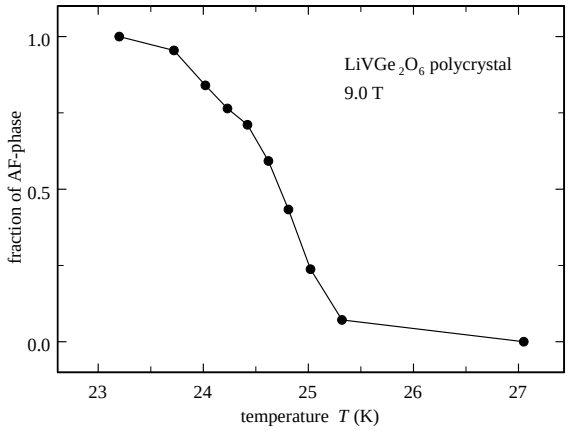

FIG. 3: Fraction of the total NMR intensity in the polycrystalline $LiVGe_2O_6$ spectra at 9.0 Tesla which is attributed to the antiferromagnetic phase.

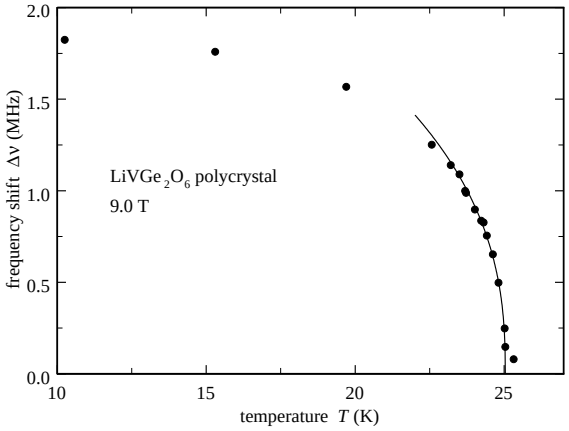

FIG. 4: Frequency shift $\Delta\nu$ from the NMR spectra of polycrystalline $LiVGe_2O_6$. The width in the paramagnetic phase at 26 K has been subtracted. The solid line is a fit to the data (see text).

broad, nearly rectangular shape. This shape is expected for a randomly oriented powder spectrum if $\mathbf{B}_\mathrm{i}$ has the same magnitude at all ^{7}Li nuclei, is parallel or antiparallel to a single crystalline direction and maintains the same orientation with respect to the crystalline axes for all orientations of $\mathbf{B_0}$. For $B_\mathrm{i} \ll B_0$, the field at the nuclei is given by $B_0 + B_\mathrm{i}\cos(\theta)$, where θ is the polar angle in spherical coordinates. Then, the frequency shift is: $f = \gamma B_\mathrm{i}\cos(\theta)$. The probability (dN) that a particular value of θ occurs is: $dN = 1/2\sin(\theta)d\theta$ and the density of states in the powder pattern is:

$$\frac{dN}{df} = \left|\frac{dN}{d\theta}\right|\left|\frac{d\theta}{df}\right| = \frac{1}{2\gamma B_\mathrm{i}} \ , \qquad (3)$$

i.e., constant and results in a rectangular shape for the spectrum.

Since this shape is indeed observed, the powder spectra indicate that the direction of the internal magnetization is not affected by the orientation of the external magnetic field. From these measurements (see Fig. 2) we obtain the value $B_\mathrm{i} = 0.106$ T.

In Fig. 4 the part of the NMR linewidth $(\Delta\nu(T))$ proportional to the AF order parameter is plotted as a function of temperature. The contribution of the width in the paramagnetic phase is subtracted in quadrature from the AF contribution using

$$\Delta\nu = (\Delta\nu_\mathrm{AF}^2 - \Delta\nu_\mathrm{P}^2)^{1/2} \ , \qquad (4)$$

where $\Delta\nu_\mathrm{AF}$ and $\Delta\nu_\mathrm{P}$ are the HWHM of the spectra in the AF phase and in the paramagetic phase at 26 K, respectively. The solid line corresponds to a power law behavior $\Delta\nu(T) \propto (T_\mathrm{N} - T)^{0.4\pm0.05}$. The onset of the broadening of the spectra occurs at 25.04 K, which we identify as the Néel temperature T_N for the polycrystalline sample.

B. NMR spectra of $LiVGe_2O_6$ single crystals

The coordinates shown in Fig. 5 will be used to discuss our measurements on the single crystal samples. They include the crystalline axes a, b, and c, the cartesian axes x, y, and z, and the spherical coordinates θ (polar angle) and ϕ (azimuthal angle). X-ray measurements[9] have shown that the long dimension of $LiVGe_2O_6$ single crystals is along the crystallographic c-direction. For all of our single crystal NMR measurements, the value of ϕ is close to zero, unless specified otherwise.

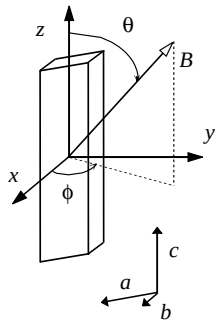

FIG. 5: Definition of various coordinates for a typical $LiVGe_2O_6$ single crystal.

Figure 6 shows NMR spectra of a $LiVGe_2O_6$ single crystal at temperatures between 23 and 26 K for $\theta \approx 60°$. The NMR spectrum is a single line in the paramagnetic

phase and two lines in the AF phase that correspond to the two magnetically inequivalent ^{7}Li sites. As for the powder spectra, both phases coexist over a small range of T. However, this range is substantially narrower with a value $\simeq 0.3$ K for the single crystal.

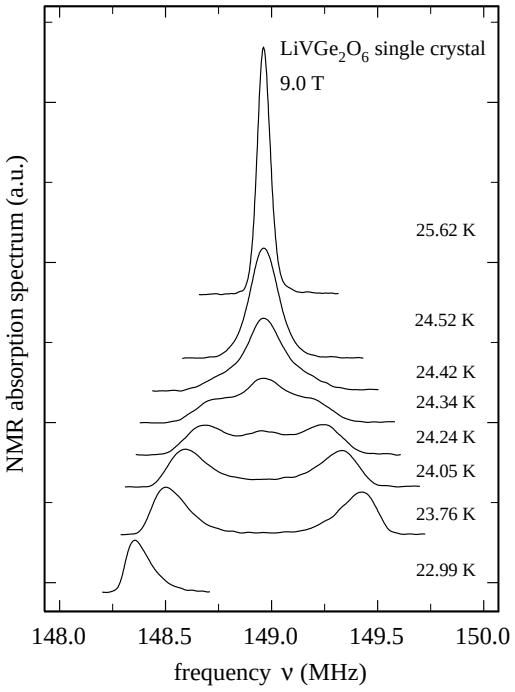

FIG. 6: Single crystal ^{7}Li NMR spectra of $LiVGe_2O_6$ near T_N. The needle direction, which corresponds to the crystallographic c-direction, is aligned 60° from the applied magnetic field.

As for the powder sample, the single crystal linewidths are rather broad near T_N. Just above the transition, $\Delta\nu(T)$ is about 36 kHz compared to 19 kHz at 38 K. Since the dc-susceptibility increases with increasing T in this range, the opposite change in the linewidth may indicate that there are slow, short range fluctuations above the phase transition that enhance the linewidth somewhat. Furthermore, in the whole considered temperature range, the linewidths of the single crystal signals are consistent with the width of the broadening function used to fit the spectra of the polycrystalline sample. The large NMR line width seen just below T_N may also be caused by a distribution of T_N in the sample.

In Fig. 7, $\Delta\nu(T)$, representing the splitting of the two peaks in the ^{7}Li NMR spectrum, is plotted as function of T for $B_0 = 9.0$, 41.5 and 44.5 T, with $\theta = 30°$ at 9.0 T and approximately 20° for the measurements at 41.5 and 44.5 T. The data obtained at 41.5 and 44.5 T have also been multiplied by 1.15 and 1.28, respectively, to bring

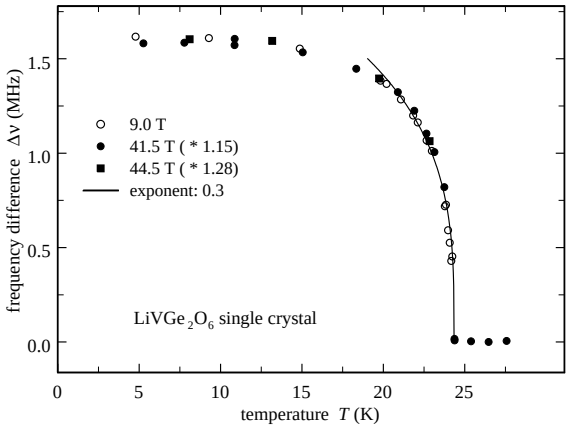

FIG. 7: Frequency shift $\Delta\nu$ of the ^{7}Li peaks in the AF phase of $LiVGe_2O_6$ from the peak in the paramagnetic phase as a function of T. For comparison, the measurements at 41.5 and 44.5 Tesla have been multiplied by the factors 1.15 and 1.28 respectively. The solid line is a fit to the data (see text).

the curves together. This indicates a somewhat reduced value of the order parameter for the measurements in higher fields, an aspect that will be discussed later. For the same reason, the values of T have been reduced by 0.6 K and 1.6 K for the measurements at 41.5 T and 44.5 T, respectively. We attribute these adjustments in T as being caused by differences in the instrumentation, which resulted in an uncertainty of about 1 K in T_N for the measurements at these higher values of B_0.

Because of the large values of B_0, a substantial reduction of T_N proportional to B_0^2 is expected.[10] However, as can be seen in Fig. 7, no such reduction is observed. This seems rather surprising because $g\mu_B B/k_B = 54$ K, for $B = 44.5$ T with $g = 1.79$, i.e., about twice T_N. It may be, however, that the value of $g = 1.79$, obtained from the paramagnetic susceptibility[1] is too large because, as will be discussed later, the measurements of Lumsden *et al.*,[3] as well as our own measurements, show that the value of the ordered moment is only about 1.14 μ_B. Furthermore, it is evident that a large change in B_0 has no significant effect on the T dependence of the order parameter in the ordered phase, as the three curves coincide. The solid line is a power law fit to the data just below the transition with $\Delta\nu(T) \propto (T_N - T)^{0.3\pm0.05}$. The value of the exponent is somewhat smaller than that 0.4 obtained for the polycrystalline sample. Qualitatively, such a reduction is consistent with the smaller distribution of T_N inferred from the smaller temperature range over which a coexistance of two phases is indicated in the single crystal samples.

C. T_1^{-1} (T, B) for polycrystalline $LiVGe_2O_6$

In this section we describe our spin-lattice relaxation rate measurements at 9.0 and 23 Tesla performed on the polycrystalline sample. Below T_N the measurements were done at the same frequency and magnetic field as above the transition. But because of the very broad linewidth of about 3.5 MHz in the AF-phase, only a small part of the NMR spectrum was covered by the RF-pulses. The nuclei near resonance were those with $\theta \approx 90°$; i.e., $\mathbf{B_0}$ close to lying in the azimuthal plane. The angle ϕ is distributed randomly over 2π.

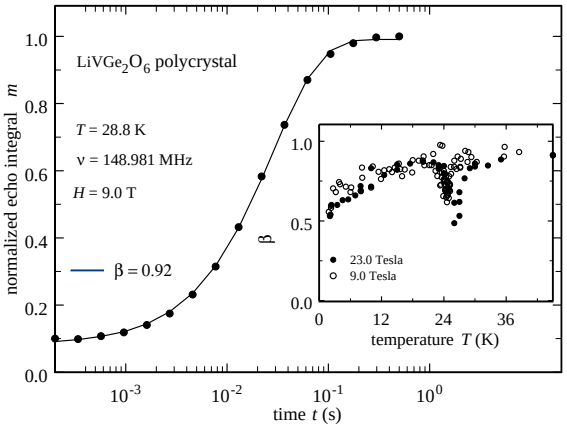

FIG. 8: Recovery of the magnetization during a T_1^{-1} measurement in polycrystalline $LiVGe_2O_6$. The solid line is the fit of Eq. 1 for $\beta = 0.92$. Inset: Plot of β as function of T at 9.0 and 23 T.

Figure 8 shows a typical magnetization recovery curve (filled circles). The best fit using Eq. 1 (solid line), which yields $\beta = 0.92$, is an excellent fit to the data. The inset of Fig. 8 shows that the T-dependence of β is essentially the same at both 9.0 T and 23.0 T. Except for T close to T_N, above 12 K the values obtained for β are close to 1 and correspond to a relatively narrow distribution of T_1^{-1}. Near the transition and below 12 K, β considerably deviates from 1, which indicates a substantially broader distribution of T_1^{-1} at these temperatures. We attribute the broadening of the distribution of T_1^{-1} close to T_N to the distribution of T_N for the different parts of the sample mentioned earlier. As discussed below for the single crystal measurements, the large deviation from $\beta = 1$ seen below 12 K reflects a large, unexpected dependence of T_1^{-1} upon ϕ.

The T_1^{-1} values obtained for 9.0 T and 23.0 T are shown in Fig. 9. Where β is substantially less than 1, a wide distribution of values for T_1^{-1} is present. Therefore, the plotted value is the one that represents the single recovery rate that characterizes this distribution. Nevertheless, from its T-dependence useful information on the dynamics of our system can be obtained, even at the lowest values of T. For the 9.0 T measurements, well above T_N, T_1^{-1} depends only weakly on T, slowly increasing by about a factor 2 between 40 and 200 K and remaining almost constant between 200 and 300 K. Therefore, as previously reported[1,2], there is no indication of a Haldane gap in this quasi 1-D system. Below 40 K, T_1^{-1} increases rapidly to a maximum value of about 140 s^{-1} at T_N, presumably due to critical fluctuations near the transition.

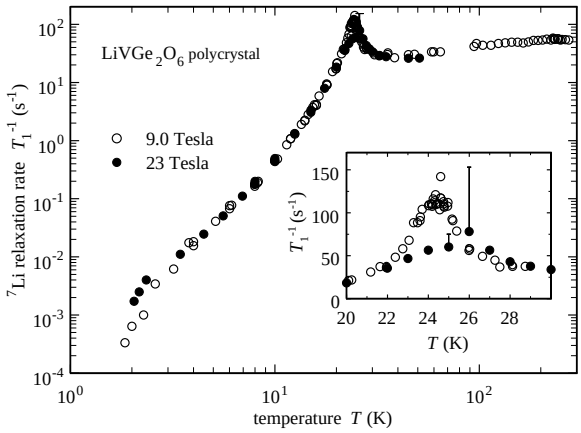

FIG. 9: ^{7}Li T_1^{-1} as function of T in polycrystalline $LiVGe_2O_6$ at 9.0 (open circles) and 23 Tesla (filled circles).

Below 23 K, T_1^{-1} drops very rapidly by about 6 decades to a value near $3 \cdot 10^{-4}$ s^{-1} at 1.8 K. In the low T regime, the effect of B_0 on $T_1^{-1}(T)$ is very weak. Because the value of $g\mu_B B/k_B$ for 23 T is close to T_N this result was unexpected, as was the small influence of B_0 on the spectra shown in Sec. III B which are also affected only weakly by B_0.

D. $T_1^{-1}(T)$ of a $LiVGe_2O_6$ single crystal

Figure 10 shows measurements of T_1^{-1} as a function of T for a single crystal of $LiVGe_2O_6$ for $\theta = 90°$, 60°, and 30°, with $\phi \sim 0°$. Over the whole temperature range, no significant deviations from $\beta = 1$ were observed. This behavior indicates that unlike the polycrystalline sample, there is no distribution in T_1^{-1}; i.e., the relaxation follows a single exponential. In principle, this result should make a detailed interpretation of the results more straightforward.

The general behavior of $T_1^{-1}(T)$ is similar to that of the polycrystalline sample. From 200 K to 40 K the relaxation rate slightly decreases by about a factor of two, but subsequently increases by more than one order of magnitude towards T_N, and decreases rapidly below T_N. The inset of Fig. 10 shows a log-log plot of T_1^{-1} for $\theta \approx 90°$ close to T_N as a function of $|T - T_N|$ with $T_N = 24.45$ K. Close to the transition, the data both

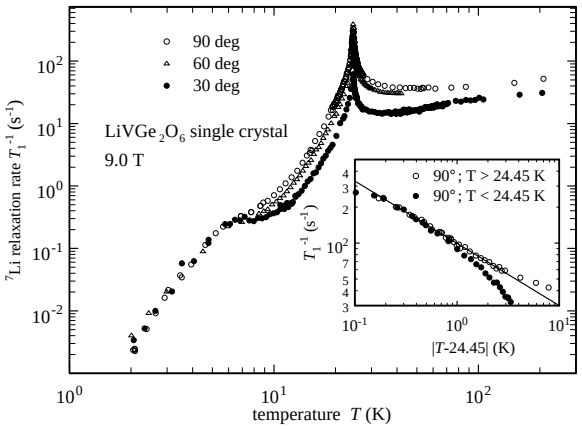

FIG. 10: ^{7}Li T_1^{-1} as function of T in a single crystal of $LiVGe_2O_6$. The three values of the polar angle θ are 90° (open circles), 60° (open triangles), and 30° (filled circles). Inset: T_1^{-1} as function of $|T-24.45|$ above (open circles) and below (filled circles) T_N for $\theta \approx 90°$.

below and above T_N, fall on the same curve, given by

$$T_1^{-1} \propto |T - 24.45|^{-0.55} \ . \qquad (5)$$

Although the exponent -0.55 is expected to reflect the critical behavior of the AF transition in this material, it should be interpreted with caution. Because the width of the transition shown by the coexistence of both phases (Fig. 6) over a range of 0.3 K may indicate a distribution of T_N in the sample, it may be that the exponent is really a lower limit on the rate of the divergence on approaching T_N.

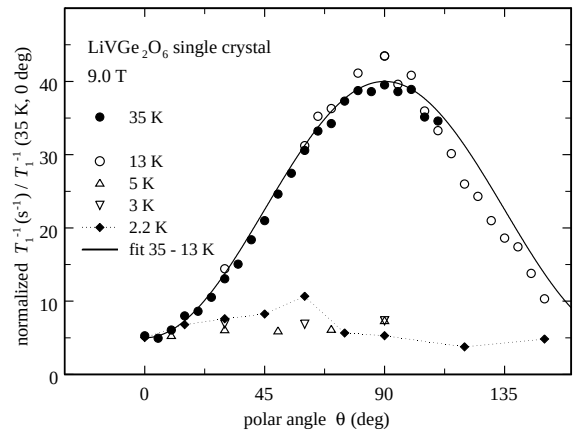

FIG. 11: Angular dependence of T_1^{-1} in a $LiVGe_2O_6$ single crystal at five temperatures between 35 and 2.2 K. The solid line is a fit to the data at 35 and 13 K (see text).

Figure 10 also shows that the θ-dependence of $T_1^{-1}(T)$ on T has a crossover from θ being approximately independent of θ below 8 K to a strong dependence above 10 K. This behavior is shown in more detail in Fig. 11, where T_1^{-1} is plotted as function of θ for several values of T both above and below 10 K. Above 10 K, T_1^{-1} is well described by

$$T_1^{-1}(\theta) = A(T)[35\sin^2(\theta) + 5] \ , \qquad (6)$$

where A determines the magnitude of T_1^{-1}. The measurements at 5 and 3 K do not show any dependence on θ. At 2.2 K, the moderate θ-dependence of T_1^{-1} is not well enough established to draw useful conclusions.

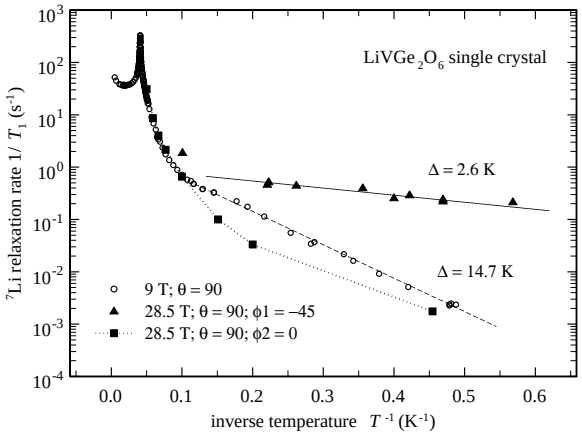

FIG. 12: ^{7}Li T_1^{-1} as function of $1/T$ in a $LiVGe_2O_6$ single crystal at 28.5 T and the polar angle $\theta = 90°$ for two azimuthal angles $\phi_1 = -45°$ (filled circles) and $\phi_2 = 0°$ (filled squares) and at 9.0 T at $\theta = 90°$ (open circles). The solid and dashed lines indicate energy gaps of 2.6 and 14.7 K respectively. The dotted line is a guide to the eye.

Now we turn to measurements in which ϕ was varied and θ is held fixed at 90°; i.e., $\mathbf{B_0}$ was rotated in the azimuthal plane. For these measurements, the direction corresponding to $\phi = 0$ is always the same, but the location of $\phi = 0$ in the azimuthal plane is not known. Figure 12 shows T_1^{-1} at $\theta = 90°$ as a function of $1/T$ for $\phi_1 = -45°$ and $\phi_2 = 0°$ at 28.5 T and, for comparison at 9.0 T and $\phi = 0°$. In addition the ϕ dependence of T_1^{-1} for 4.5 and 1.7 K at $\theta = 90°$ and 28.5 T is shown in Fig. 13. A huge change of two decades in T_1^{-1} is seen for a variation of only 30° in ϕ.

These variations of T_1^{-1} with θ and ϕ help to explain the observation that $\beta \leq 1$ throughout the entire range of T for the polycrystalline sample (Fig. 8). Below ~ 8 K, the variation of T_1^{-1} as a function of ϕ causes a very broad distribution of T_1^{-1} in the polycrystalline sample that is qualitatively consistent with the established small values of β. Similarly, above T_N, the narrower distribution of T_1^{-1} caused by its variation with θ (Fig. 10) results in a value of β that is slightly less than one. In the range 10-20 K, the moderate range of θ near 90° selected by the

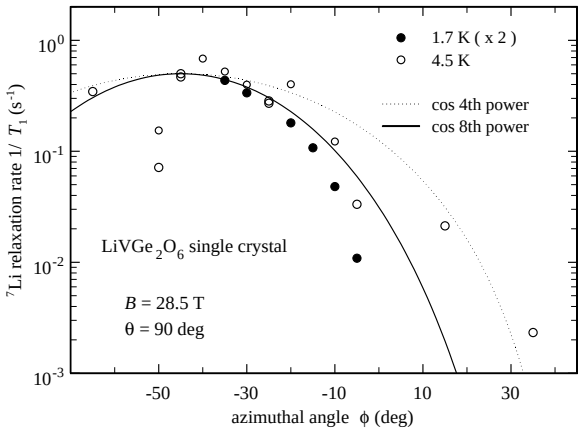

FIG. 13: ^{7}Li T_1^{-1} as function of ϕ in a $LiVGe_2O_6$ single crystal at 28.5 T and $\theta = 90°$ for $T = 4.5$ K (open circles) and $T = 1.7$ K (filled circles).

rf pulse at the center of the spectrum and the variation of T_N in the sample are probably the major conditions responsible for the measured value of β.

Our T_1^{-1} measurements at the highest B_0 of 41.5 T for a limited number of angles and temperatures are shown in Fig. 14 and its inset. No significant deviation from the results at lower B_0 is evident. This behavior shows that although the dynamical properties of the electron moments that form the AF state are quite sensitive to the alignment of $\mathbf{B_0}$, they are nearly independent of its magnitude up to 41.5 T.

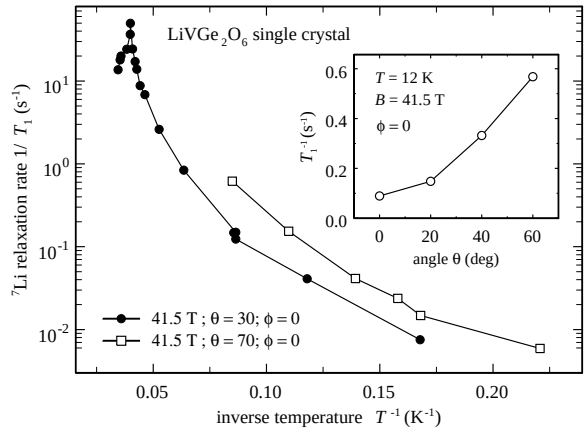

FIG. 14: ^{7}Li T_1^{-1} as function of $1/T$ in a $LiVGe_2O_6$ single crystal at 41.5 T for $\theta = 30°$ (solid circles) and $\theta = 70°$ (open squares. Inset: θ-dependence of T_1^{-1} at 12 K and 41.5 T.

E. $T_2^{-1}(T)$ of $LiVGe_2O_6$

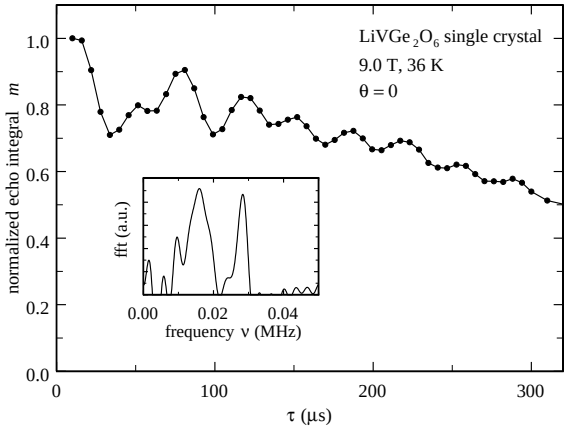

FIG. 15: Spin-echo decay as a function of τ in a $LiVGe_2O_6$ single crystal at 9.0 Tesla. Inset: FFT of the spin-echo decay.

Figure 15 shows the oscillatory behavior of the amplitude of the spin-echo decay as a function of the pulse spacing τ at 9.0 T, 36 K, and $\theta = 0$ in a single crystal sample. We attribute the modulation of the echo height to the static quadrupole interaction of the ^{7}Li nuclei. From the period of the modulation, τ_m, the quadrupole frequency, ν_Q, is obtained:[11] $\nu_Q = 1/\tau_m$. Since the orientation of the electric field gradient (EFG) tensor at these sites is not known, our limited measurements do not provide an exact value of ν_Q. However, from the fourier transform of the decay curve for a T_2 measurement with one of the shortest periods (see inset Fig.15), an approximate value of $\nu_Q \approx 15$ kHz is obtained for the quadrupole frequency. Actually, two frequencies ν_Q and $2\nu_Q$ are seen, as expected for a nuclear spin $I = 3/2$ system.[11] Also no change in the modulation was observed over the entire range of T that was covered. This behavior indicates that the EFG is constant and that no structural change occurs at T_N, in agreement with neutron and x-ray diffraction measurements.[3]

In Fig. 16, T_2^{-1} as function T is plotted at $B_0 = 9.0$ T for both a polycrystalline powder sample and a single crystal sample. Several features are seen in these measurements. Except for very close to the transition, $T_2^{-1} \simeq 1000$ s^{-1} above T_N. Also, there is a narrow peak in T_2^{-1} within 1 K of T_N in which T_2^{-1} is enhanced by about 25 % for the powder sample and by 70 % for the single crystal one. We attribute these increases to slow, critical fluctuations, of the local field near T_N.

As T decreases below 23 K, there is an increase in T_2^{-1} by the factor 2.3. From elementary considerations, one might expect a *reduction* in T_2^{-1} caused by the AF field "detuning" the ^{7}Li spins. Although it should be present, this mechanism is clearly not the dominant one for T_2^{-1}. There are three mechanisms that are often responsible

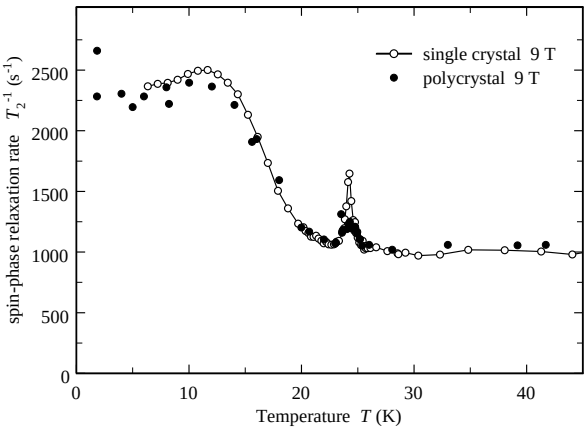

FIG. 16: ^{7}Li T_2^{-1} as function of T at 9.0 T in polycrystalline $LiVGe_2O_6$ (filled circles) and a $LiVGe_2O_6$ single crystal (open circles).

for such an increase in T_2^{-1}: (1) A slow fluctuation of the local magnetic field or EFG in the frequency range near to T_2^{-1}, (2) an increase in T_1^{-1} to values on the order of or larger than T_2^{-1} caused by other mechanisms, or (3) an enhancement of the spin-spin interactions between the nuclei being measured. We expect that the first is not determining T_2^{-1} because it seems unlikely that slow fluctuations would be independent of T when the fast ones that determine T_1^{-1} vary so rapidly with T. The second obviously does not apply because all of the measured values of T_1^{-1} are too small. It may be that the third mechanism does apply through the ^{7}Li-^{7}Li spin-spin interaction being enhanced by the Suhl-Nakamura interaction mediated by the AF spin wave modes[12] that are expected to form at low T. Although this approach shows some promise, to evaluate it in detail is beyond the scope of this paper.

IV. DISCUSSION

In this Section, we discuss and interpret features of our results that have not been covered in the above presentation of the data.

A. Magnetic structure

In this Section we discuss how the NMR spectra of both the powdered and the single crystal samples can be used to infer the spatial arrangement of the moments in the AF phase of $LiVGe_2O_6$. First, we consider what can be inferred from the data in the randomly oriented polycrystalline sample. Its NMR spectra in the AF phase can be analyzed in a similar way as in the paramagnetic phase (see Sec. III A); i.e. sum the contribution of all the V^{3+} ions in a sphere of about 5nm around the ^{7}Li nuclei, but with the magnetic moments on the V^{3+} ions having an AF configuration. We used the AF structure corresponding to a simple AF period along the chains, a ferromagnetic order between the chains and a value of 1.14 μ_B for the magnetic moments reported by Lumsden et al.,[3] but with several different orientations of the magnetic moments. For the moments pointing along the (100) direction, a total field of only 0.022 T, which is much less than the measured value of about 0.106 Tesla (see Sec. III A), is obtained. However, when the moments are parallel to the (001) direction, the result is 0.104 T, which is very close to the measured value. Thus, the polycrystal measurements are compatible with the proposed AF structure by Lumsden et al.[3], but with the magnetic moments pointing along the crystallographic c-direction instead of the a-direction.

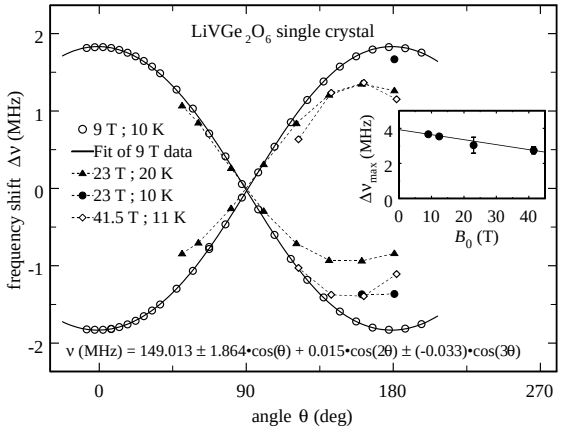

FIG. 17: Shift of the ^{7}Li NMR-absorption peaks in $LiVGe_2O_6$ as function of θ at 9.0, 23.0 and 41.5 T. The solid lines are fits to the data at 9.0 Tesla (see text) and the dashed lines are guides to the eye. Inset: Frequency difference $\Delta\nu$ between the two NMR lines in the AF phase, as function of B_0 at $T \approx 10$ K. The solid line is a guide to the eye.

The measurements on the single crystal samples provide even more direct evidence that the hyperfine fields at the Li sites, and therefore the moments on the V^{3+} ions, are aligned parallel (and antiparallel) along the crystallographic c-direction. This can be seen from Fig. 17, where $\Delta\nu$ for the two peaks in the ^{7}Li spectrum caused by the magnetically inequivalent sites in the AF phase near 10 K is plotted as function of θ. For the measurements at 9.0 T, a good fit to $\Delta\nu$ is given by:

$$\Delta\nu = 149.01 \pm 1.86\cos(\theta) + 0.01\cos(2\theta) \mp 0.03\cos(3\theta). \quad (7)$$

The dominant term in this fit is proportional to $\cos(\theta)$, which is consistent with $\mathbf{B}_i$ being parallel to the c-axis for all values of θ. Since $\mathbf{B}_i$ has this orientation for the AF ordered moments parallel to the c-axis, we conclude that the moments themselves are aligned with the c-axis

in the AF phase.

For the measurements at 9.0 T, the deviations from the cosine function are quite small. The $\cos(2\theta)$ dependence can be interpreted as a slight tipping of the moments by $\mathbf{B_0}$.[13] The inset of Fig. 17 shows the maximum shift $\Delta\nu_{\max}$ as a function of B_0 at $T \approx 10$ K. The few high field measurements near 10 K indicate a small reduction of the order parameter. Because of the small number of measurements, this point needs confirmation by a more complete set of measurements.

B. Phase transition

As shown in Sec. III A, the NMR spectra of the polycrystalline sample indicate the coexistence of the paramagnetic and AF phases over a range of 1.5 K, centered around $T_{\rm N}$. It has been suggested[2] that a first order transition is responsible for the coexistence of the two phases. On the other hand the T-dependence of the splitting, which is proportional to the order parameter, varies continuously and smoothly to zero at the transition temperature. This behavior indicates that the phase transition is of second order, or at most, very weakly first order. An alternative explanation for the coexistence of the two phases is a distribution of transition temperatures $T_{\rm N}$. Such a distribution, caused by dislocations, stacking faults and V vacancies, could easily be present in a polycrystalline sample. This explanation is also consistent with the small value of the exponent β near the transition (inset of Fig. 8), which indicates a very broad distribution of T_1^{-1} about $T_{\rm N}$, where T_1^{-1} varies more rapidly with T than at temperatures nearby. The variation of T_1^{-1} with T very close to the transition (inset, Fig. 9) is slower than expected given the divergent critical behavior near a second order transition. As indicated earlier, this suppression of the critical divergence could be caused by a distribution of $T_{\rm N}$.

This interpretation in terms of a distribution of $T_{\rm N}$ is supported by our measurements on single crystals. In comparison with the polycrystalline sample, the data imply a coexistence of both phases over the substantially narrower range of about 0.3 K and a peak in T_1^{-1} that is narrower and higher near $T_{\rm N}$ (inset, Fig. 10). This behavior is qualitatively consistent with a distribution of $T_{\rm N}$ in which the single crystal has fewer imperfections and therefore a more narrow distribution of $T_{\rm N}$ than the polycrystalline sample.

In Sec. IV A it was shown that the AF state of $LiVGe_2O_6$ has a rather simple magnetic structure. It has, however, some unusual features which we turn to now. First, consider the magnitude of $T_{\rm N}$. We start with a simple spin Hamiltonian which, as will be discussed later might not be sufficient to describe the system:

$$H = J_{\parallel} \sum_{\langle i,j \rangle} S_i \cdot S_j + D \sum_j (S_j^z)^2 + J_{\perp} \sum_{(i,j)} S_i \cdot S_j \ , \quad (8)$$

where $\langle i,j \rangle$ denotes an intrachain nearest-neighbor pair and (i,j) denotes an intrachain one. $J_{\parallel}$ and $J_{\perp}$ are respectively the the intrachain and interchain coupling constants, and D is the single-ion anisotropy. The value about 45 K has been estimated for $J_{\parallel}$.[1,2] Because of the quasi 1-D character of the crystal structure, it is surprising that the measured value $T_{\rm N} \sim 25$ K could be more than half $J_{\parallel}$. On the basis of a mean-field calculation[14] and the assumptions $J_{\parallel} = 45$ K, four neighboring chains, and $T_{\rm N} = 25$ K, $J_{\perp}$ has been estimated[3] to be about 1.4 K, or $[J_{\perp}/J_{\parallel}] \simeq 0.03$. More advanced calculations[15,16,17] show, however, that such a ratio is barely enough to induce an AF transition, and very unlikely to have a value of $T_{\rm N}$ as large as $J_{\parallel}/2$. In fact based on the calculation of Sénéchal et al.[16] we estimate the ratio of the interchain to the intrachain coupling constant which would be needed to explain the relatively high transition temperature to be larger than 0.06. From crystal considerations, however, this value seems to be very large. For example, $AgVP_2S_6$, which is a compound with a structure similar to $LiVGe_2O_6$, has a ratio $J_{\perp}/J_{\parallel} \leq 10^{-5}$.[18] Therefore, it seems that the relatively high transition temperature cannot be explained by the interchain coupling alone. If, however, the Haldane gap is not present, even a very small coupling between the chains might be enough to induce an AF phase transition. Later, we will consider this possibility in terms of a large single-ion anisotropy.

Another remarkable feature of $LiVGe_2O_6$ is the weak influence of B_0 on the properties of the AF state. This applies to $T_{\rm N}$, is seen in the properties of an apparent gap in the fluctuations responsible for T_1^{-1} (to be discussed later), and is evident in the absence of a spin-flop transition for B_0 as high as 44.5 T. The last point is noteworthy because on the basis of a simple mean-field approximation, the spin-flop field ($H_{\rm SF}$) is expected to be[19]

$$H_{\rm SF} = (2H_{\rm E}H_{\rm A} - H_{\rm A}^2)^{1/2} \ , \quad (9)$$

where $H_{\rm A}$ is the anisotropy field and $H_{\rm E}$ is the exchange field. The field $H_{\rm A}$ is related to the single-ion anisotropy according to $D = H_{\rm A} g \mu_{\rm B}/S$. From these considerations, $D > 50$ K, which might be responsible for closing the Haldane gap[20] and may explain the relatively high AF-phase transition temperature $T_{\rm N}$. Although the mean-field approximation used here might not be fully appropriate because $H_{\rm A}$ is comparable to $H_{\rm E}$, it does allow us to obtain at least a rough estimate of the single-ion anisotropy using the Hamiltonian of Eq. 8.

It should be pointed out that according to a recent publication,[6] no phase transition is expected to occur in $LiVGe_2O_6$. In this work, mid-gap states are assumed to be responsible for the susceptibility anomaly in the experimental data of $LiVGe_2O_6$ and it is predicted that this anomaly will be weaker if their are fewer crystal defects and non-magnetic impurities. This interpretation is in clear contradiction with the prior NMR[2] and neutron diffraction[3] experiments and our NMR measurements reported here. Our experiments on both polycrystalline

and high quality single crystal samples show clearly that a magnetic phase transition occurs and permit us to refine the magnetic structure proposed earlier.[3] Although the phase transition appears to be more complicated than a simple ordering driven by inter- and intrachain coupling, there is no doubt that the V moments order antiferromagnetically below approximately 25 K.

C. T_1^{-1} as function of T,B, θ and ϕ

Although in principle part of the coupling responsible for T_1^{-1} of the ^{7}Li spins could be quadrupolar, the discussion in the next paragraph argues that there is no significant quadrupolar contribution to it. As a result, our interpretation of T_1^{-1} involves only magnetic coupling to the ^{7}Li spins.

There are basically two mechanisms for electric field gradient fluctuations that might contribute to T_1^{-1} of the ^{7}Li spins: Charge fluctuations associated with some instability of the lattice and the Raman-type phonon process first described by van Kranendonk.[21] Since the quadrupolar splitting found in Sec. III E is very small and does not change over the temperature range studied, there is no reason to expect a significant contribution to T_1^{-1} from charge fluctuations. Also, the small ^{7}Li quadrupolar interaction and observed T-dependence of T_1^{-1} rule out quadrupolar relaxation by phonons.[21] We therefore conclude that there is no significant quadrupolar contribution to T_1^{-1} and that it is caused by magnetic fluctuations.

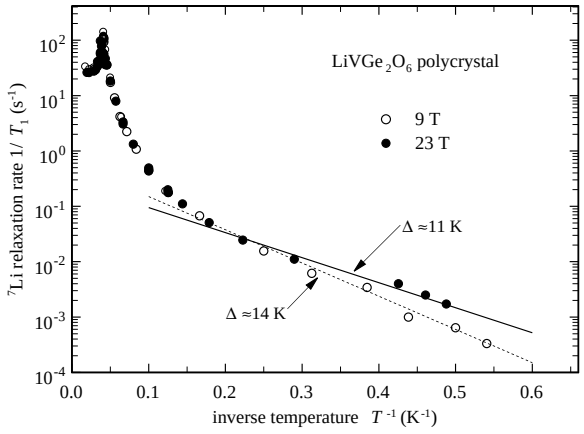

FIG. 18: ^{7}Li T_1^{-1} as function $1/T$ in polycrystalline $LiVGe_2O_6$ at 9.0 and 23 T. The solid dashed lines are fits to the low T data using Eq. 10. The values shown for Δ are 14 K at 9 T and and 11 K at 23 T.

In Fig. 18 the spin-lattice relaxation rate, T_1^{-1}, of polycrystalline $LiVGe_2O_6$ is plotted as function of T^{-1} for $B_0 = 9.0$ T and 23 T. Well into the AF phase below 10 K, the behavior of T_1^{-1} has the T-dependence expected of electron spin excitations across an energy gap (Δ); i.e. the slope of the curve is constant and negative at low T. If one simply fits the data to

$$T_1^{-1}(T) \propto \exp(-\Delta/T) \ , \tag{10}$$

the values obtained for Δ are 14 K at 9.0 T and 11 K at 23 T.

Such values must, however, be interpreted as an average over a distribution of Δ that is quite broad. This is seen in Fig 12, where there is a large variation of the slope for two different values of ϕ at 28.5 T (solid lines), and a large slope at 9 T and $\phi \simeq 0$ (dashed). The two values Δ =2.6 K and Δ =14.7 K indicate a very large effect of the alignment of B_0 in the azimuthal plane on Δ for magnetic excitations at low T. Therefore, the following discussion of the polycrystalline sample results applies to an average behavior and is approximate and phenomenological.

First, consider the effect of B_0 on Δ. In a 3-d antiferromagnet, when there is a gap in the excitation spectrum, it usually depends strongly on B_0 because of the Zeeman interaction, which is $\propto g\mu_B B_0$. Instead, our measurements show the very weak field dependence of less than 3 K for a difference in applied field of 14 Tesla. Since $g\mu_{\rm B}B/k_{\rm B}$, with $g = 1.79$, is about 28 K for $B = 23$ T, the usual expectations for the dependence of Δ on B_0 do not apply.

Also, in comparison to our results in Sec. IV B, Δ appears too small to be attributed to a magnon gap. From $\Delta = 14$ K and 11 K at 9.0 T and 23 T respectively, one would expect a $\Delta \simeq 16$ K. From this value, a spin-flop field smaller than 20 T is expected, which is contradicted by the absence of a spin-flop transition up to 44.5 T shown by our NMR-spectrum measurements. On the basis of this evidence, it appears that at low T the magnetic fluctuations responsible for T_1^{-1} in $LiVGe_2O_6$ are not simple magnon excitations. This is particularly evident from the T_1^{-1} measurements shown in Figs. 12 and 13, where very large anisotropies in T_1^{-1} are seen.

It is rather difficult to identify the microscopic mechanism responsible for the very large anisotropy of T_1^{-1} shown in Fig. 13, where, for comparison, the variation $\cos^4\phi$ and $\cos^8\phi$ are shown by the dashed and solid lines, respectively. For example, if it were caused by a fluctuating magnetic field aligned with the value of ϕ corresponding to the maximum in T_1^{-1}, for other values of ϕ, one would expect the much weaker angular variation $T_1^{-1} \propto \cos^2\phi$. Similar arguments for quadrupolar relaxation (excluded above from other arguments) by a fluctuating EFG could give a variation up to $\cos^4\phi$.

Although we do not have a microscopic model for it, the temperature and angular variations seen in Figs. 12 and 13 suggest a gap-type behavior with a splitting which itself is very anisotropic. More work, both experimental and theoretical, is needed to identify the mechanisms for this behavior.

In summary, the angular dependence of the spin-lattice relaxation rate measurements for the single crystal sam-

ples is rather complicated and it is difficult to construct a detailed interpretation. For both the paramagnetic regime and the AF regime down to about 8 K, T_1^{-1} Fig. 11 and Eq. 6 indicate that the largest contribution to T_1^{-1} has the angular dependence $\propto \sin^2\theta$. This behavior is consistent with magnetic fluctuations that are predominantly along the c-direction that have dipolar coupling and only a small isotropic contribution. It may reflect primarily amplitude fluctuations of the AF order parameter.

Below about 8 K, the disappearance of the θ-dependence of T_1^{-1} and the emergence of its ϕ-dependence indicates that at low T, the origin of the fluctuations responsible for T_1^{-1} is very different from what it is at higher T.

D. Orbital degrees of freedom and magnetic anisotropy

In this section we mention some points about the magnetic anisotropy and the orbital degrees of freedom of the V electrons in $LiVGe_2O_6$ suggested by our measurements. They suggest that the second order splitting Δ_{CF} of the t_{2g} orbitals is rather small, with the consequence that (i) there is a large uniaxial anisotropy as $g_\perp = 2(1-\lambda/\Delta_{CF})$ (λ = spin-orbit coupling) is strongly reduced for small values of Δ_{CF}, and (ii) orbital fluctuations may play a significant role in the properties of T_1^{-1}.

A large anisotropy energy has not yet been observed directly from ^{51}V NMR measurements because we were not able to observe the signal. It can, however, be inferred from several aspects of our ^{7}Li NMR measurements. In particular, the absence of a significant B_0-dependence of T_N (Fig. 7), the absence of a spin-flop transition for B_0 up to 44.5 T, and the θ dependence of $\Delta\nu$ (Fig. 17) all indicate a large uniaxial anisotropy for the static magnetization. A similar picture emerges from the T_1^{-1} measurements above about 8 K, where the θ-dependence of T_1^{-1} (Fig. 11) indicates that the fluctuations of the V moments are constrained mainly to the c-direction.

The situation of the V ions in $LiVGe_2O_6$ is similar to those in V_2O_3, where it has been reported[22] that, at least for the metallic phase, T_1^{-1} at the V sites is dominated by orbital fluctuations. In $LiVGe_2O_6$ the presence of orbital fluctuations of the V^{3+} t_{2g} orbitals is suggested by the azimuthal ϕ dependence of the spin-lattice relaxation rate at the ^{7}Li site (Figs. 12 and 13) which is very anisotropic and independent of the magnitude of B_0. Furthermore, orbital fluctuations might be very effective at the ^{51}V site itself, and may be responsible for the absence of the ^{51}V NMR signal.

According to a quantum chemistry analysis of $LiVGe_2O_6$,[1,2] if Δ_{CF} between the V^{3+} orbitals is similar to the hopping integrals between neighboring V sites, it is not possible to describe the system with a pure spin Hamiltonian and the orbital degrees of freedom have to be included explicitly. Our NMR data indicate that this is the case in $LiVGe_2O_6$. Therefore, the Hamiltonian given in Eq. 8 should be modified to better describe the physics of $LiVGe_2O_6$, and include orbital degrees of freedom which might or might not be strongly coupled to the spin degrees of freedom.

V. CONCLUSIONS

We have presented pulsed ^{7}Li NMR measurements in polycrystalline and single crystal samples of the quasi one-dimensional antiferromagnet $LiVGe_2O_6$ over the B_0 and T ranges 9-44.5 T and 1.5-300 K respectively. They cover both the paramagnetic and the AF phases, for which the transition is at $T_N \simeq 24.5$ K. The measurements include NMR spectra and the relaxation times T_1^{-1} and T_2^{-1}, often as a function of alignment of B_0. From the spectrum measurements, we find that in the AF phase the magnetic structure is consistent with that reported on the basis of neutron diffraction measurements,[3] but with the moments aligned parallel to the c-axis. Measurements of T_2^{-1} show oscillations caused by the static electric field gradient. The corresponding interaction is quite small and independent of T, which indicates that over the range of T that was covered, no lattice structural transition is observed in $LiVGe_2O_6$. The spectrum measurements also provide the T-dependence of the order parameter and show that the transition is either second order or weakly first order. The coexistence of the two phases over a narrow range around T_N and the behavior of the NMR linewidth below it is attributed to a distribution of T_N in the samples. Both the spectra and the angular dependence of T_1^{-1} indicate that the external field has at most a small effect on the alignment of the AF moment. There is no spin-flop transition up to 44.5 T. These features show that there is a very large anisotropy energy in this material and that the Hamiltonian should include orbital degrees of freedom to adequately describe it. Below 8 K, a rapid dependence of T_1^{-1} on the azimuthal angle suggests the presence of a low energy gap for magnetic fluctuations that is highly anisotropic.

VI. ACKNOWLEDGEMENTS

The UCLA part of the work was supported by NSF Grants DMR-0072524. Work performed at the National High Magnetic Field Laboratory was supported by the National Science Foundation under Cooperative Agreement No. DMR-9527035 and the State of Florida. One of us (A.G.) was supported by the National Institute for Materials Science, Tsukuba, Ibaraki, 305-0003 Japan.

[1] P. Millet, F. Mila, F. C. Zhang, M. Mambrini, A. B. Van Oosten, V. A. Pashchenko, A. Sulpice, and A. Stepanov, Phys. Rev. Lett. **83**, 4176 (1999).

[2] J. L. Gavilano, S. Mushkolaj, H. R. Ott, P. Millet, and F. Mila, Phys. Rev. Lett. **85**, 409 (2000).

[3] M. D. Lumsden, G. E. Granroth, D. Mandrus, S. E. Nagler, J. R. Thompson, J. P. Castellan, and B. D. Gaulin, Phys. Rev. B. **62**, R9244 (2000).

[4] F. Mila and F. C. Zhang, Eur. Phys. J. B **16**, 7 (2000).

[5] J. Lou, T. Xiang, and Z. Su, Phys. Rev. Lett. **85**, 2380 (2000).

[6] L. Yichang, S. Liqun, H. Inoue, and S. Qin, Phys. Rev. B. **63**, 134428 (2001).

[7] W. G. Clark, M. E. Hanson, F. Lefloch, and P. Ségransan, Rev. Sci. Instrum. **66**, 2453 (1995).

[8] G. S. Carter, L. H. Bennett, and D. J. Kahan, volume 20 of *Progress in Materials Science*, Pergamon Press, Oxford (1977).

[9] S. Ravy and A. Thiollet, private comm. (2001).

[10] Y. Shapira and S. Foner, Phys. Rev. B. **1**, 3083 (1970).

[11] H. Abe, H. Yasuoka, and A. Hirai, J. Phys. Soc. Japan **21**, 77 (1966).

[12] D. Hone, V. Jaccarino, T. Ngwe, and P. Pincus, Phys. Rev. **186**, 291 (1969).

[13] T. Nagamiya, K. Yosida, and R. Kubo, Advan. Phys. **4**, 1 (1955).

[14] D. J. Scalapino, Y. Imry, and P. Pincus, Phys. Rev. B. **11**, 2042 (1975).

[15] T. Sakai and M. Takahashi, Phys. Rev. B. **42**, 4537 (1990).

[16] D. Sénéchal, Phys. Rev. B. **48**, 15880 (1993).

[17] A. Koga and N. Kawakami, Phys. Rev. B. **61**, 6133 (2000).

[18] H. Mutka, C. Payen, P. Molinié, J. L. Soubeyroux, P. Colombet, and A. D. Taylor, Phys. Rev. Lett. **67**, 497 (1991).

[19] S. Foner, in *Magnetism I*, ed. G. Rado and H. Suhl, p. 383, New York and London: Academic Press (1963).

[20] H. J. Schulz and T. Ziman, Phys. Rev. B. **33**, 6545 (1986).

[21] J. V. Kranendonk, Physica (Utrecht) **20**, 781 (1954).

[22] M. Takigawa, E. T. Ahrens, and Y. Ueda, Phys. Rev. Lett. **76**, 283 (1996).